

Correspondence

Unlock Characteristics of a Phase-Locked Loop

The dynamic lock characteristics of a phase-locked loop have been investigated by Viterbi [1]. If the equation describing a general phase-locked system (see Fig. 1) is written, the output of the phase detector is

$$e_d = K_0 \sin \phi = \frac{C_1 C_2}{2} \sin$$

$$\left[\phi_s(t) - \omega_c t - \frac{K_0 K_1 K_2 F(p)}{p} \sin \phi \right]$$

where

- C_1 is the input signal amplitude (volts),
- ϕ_s is the input signal phase (radians),
- e_d is the phase comparator output voltage (volts),
- K_0 is the phase comparator gain (volts/radian),
- ϕ is the phase difference between signal and voltage controlled oscillator (VCO) (radians),
- K_1 is the loop filter gain constant,
- $F(p)$ is the loop filter transfer function in differential operator notation ($p = \partial/\partial t$),
- K_2 is the VCO gain (radians/sec/volt),
- C_2 is the VCO output amplitude (volts),

and

ω_c is the center angular frequency of VCO (radians/sec).

Differentiating the arguments of both sides of the equation yields the general phase-locked loop equation

$$\frac{\partial \phi}{\partial t} + KF(p) \sin \phi = \frac{\partial \phi_c}{\partial t} - \omega_c \quad (1)$$

where $K = K_0 K_1 K_2$ is the overall loop gain in radians/sec. Equation (1) can be used to analyze a second order loop tracking an FM signal [2].

Assuming the loop filter to be an RC integrating circuit, the criterion for continuous tracking can be shown to be

$$\Delta \omega \leq \frac{\alpha}{(\alpha^2 + \omega_m^2)^{1/2}} \quad (2)$$

where $\Delta \omega$ is the maximum angular frequency deviation, α is the angular cutoff frequency of the loop filter, and ω_m is the angular frequency of the modulating signal. However, even if condition (2) is not satisfied continuously, partial phase-locking can be obtained, i.e., the loop will be locked during those portions of a modulating cycle in which the frequency deviation is less than the maximum value provided that the lock-in time is sufficiently short.

Manuscript received June 1, 1965. This work is a part of one of the authors' (P.H.A.) M.A.Sc. thesis. This work was supported by the National Research Council of Canada through an Operating Grant to one of the authors (S.N.K.) and a Bursary to the other author (P.H.A.).

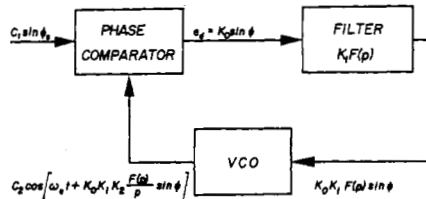


Fig. 1. The general phase-locked loop.

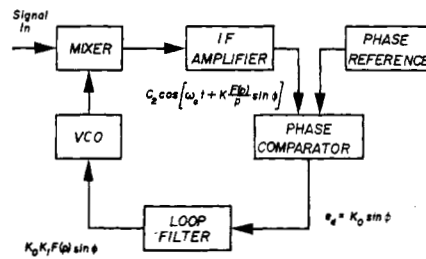


Fig. 2. Block diagram of actual phase-locked loop.

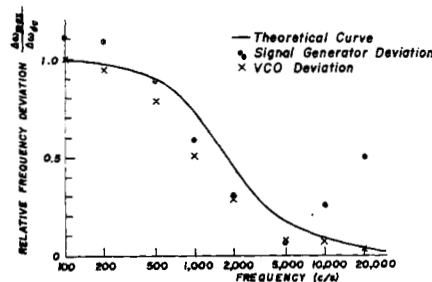


Fig. 3. Maximum dynamic lock range characteristic.

In Fig. 2 is shown a diagram of the experimental system on which the previous results for the case of continuous tracking were confirmed. The VCO is a 70 Mc/s tunnel diode oscillator which has a voltage-variable capacitor in the tank circuit. A transistor amplifier follows the oscillator and the amplified output is mixed with the incoming 100 Mc/s signal to produce a 30 Mc/s intermediate frequency. This arrangement does not change the essential character of the loop, but provides a convenient method of obtaining high loop gain and allows the principles developed to have quite general applicability.

A graph of (2) as well as the experimentally obtained points are illustrated in Fig. 3. The normalized maximum angular frequency deviation is plotted against the audio modulating frequency. The normalization constant $\Delta \omega_{dc}$ is the static tracking range of the loop. The values obtained were measured at the signal generator by means of an internal frequency deviation meter, and at the VCO output with a calibrated FM receiver. Since the frequency deviation meter calibration was not checked, the agreement between the theoretical curve

and the experimental points is felt to be within the limitations of the equipment.

Throughout the preceding analysis, the presence of noise has been ignored. A signal-to-noise ratio of about 30 dB was used during the measurements. The case involving low signal-to-noise ratios is presently being investigated.

PHILIP H. ALEXANDER
SURINDRA N. KALRA
Dept. of Elec. Engrg.
University of Windsor
Windsor, Ontario, Canada

REFERENCES

- [1] A. J. Viterbi, "Acquisition and tracking behaviour of phase-locked loops," *Proc. Symp. on Networks and Feedback Systems*, Polytechnic Inst. of Brooklyn, N. Y., pp. 583-619, April, 1960.
- [2] P. H. Alexander, "A tunnel diode phase-locked oscillator," M.A.Sc. Thesis, Univ. of Windsor, Windsor, Ontario, October, 1964.

The Short-Backfire Antenna

Backfire antennas discussed, [1] to [6], are characterized by the multiple reflection of electromagnetic waves between two plane reflectors of different size, with the energy being bound to the longitudinal antenna axis by a slow wave structure. A sketch of a typical backfire antenna is shown in Fig. 1; M marks the larger, R the smaller of the two plane reflectors that are arranged parallel to each other and transverse to the longitudinal antenna axis. The D 's indicate a row of dipole elements that constitutes the slow wave structure. The spacing L between the plane reflectors M and R is also the total axial length of the backfire antenna.

The open region between the plane reflectors acts similarly to a laser cavity [5], [6], with a standing-wave field distribution along the axis. The energy is radiated off through the aperture plane VV which passes through reflector R . Optimized conditions, which include optimum adjustment of height and spacing of the dipole elements D as well as of the size of the reflectors M and R , yield a gain increase of 6 dB above an equal-length endfire antenna. For larger backfire antennas an even higher increase in gain is possible if stacked reflectors are used [5], [6].

Until very recently, only backfire antennas that were at least one wavelength long had been investigated. As a result of more recent work, however, an even shorter backfire antenna—in fact, the shortest one at all conceivable (approximately 0.5λ long)—has awakened an interest all its own. This "short-backfire" antenna is so com-

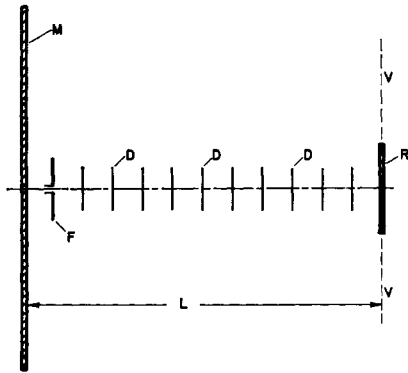
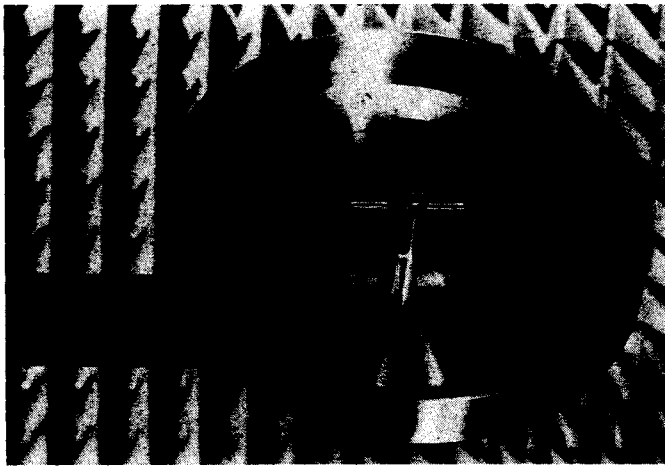
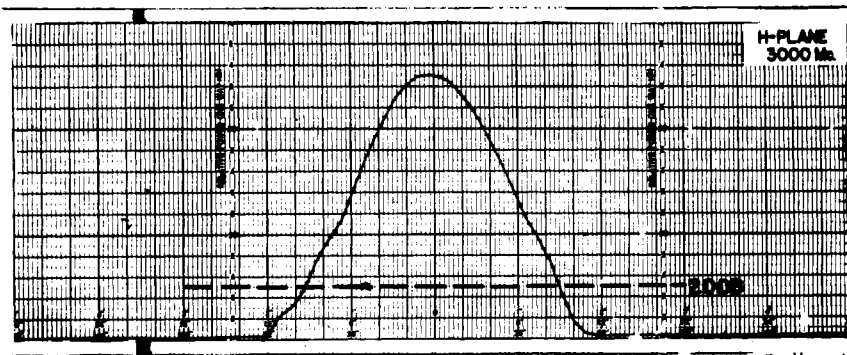
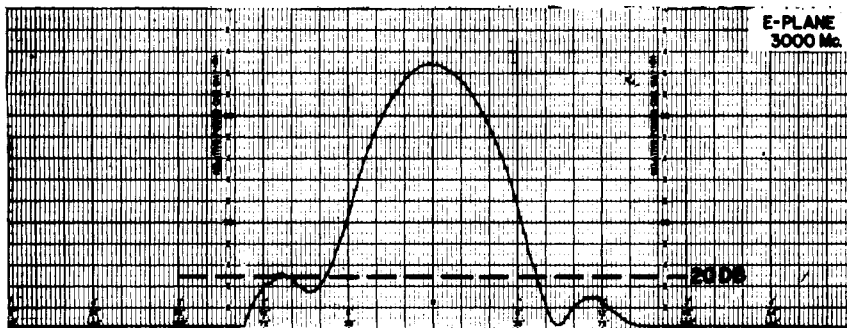


Fig. 1. Backfire antenna structure.



(a)



(b)

Fig. 2. S-band model of short-backfire antenna. (a) Antenna structure. (b) *E*- and *H*-plane pattern for 3000 MHz.

fact that practically all of the energy radiated into the cavity is intercepted by reflectors *M* and *R*. Over such a short distance, a slow-wave structure would be of no help in trapping the energy, and is therefore not used. The new antenna thus consists of only the plane reflectors *M* and *R*, spaced approximately half a wavelength apart, and the feed between them. Although its basic structure is still recognizably that of the backfire antenna, the short-backfire antenna differs so noticeably in design principles and specific constructions described, [1] to [6], as to justify a special name.

A photograph of an S-band short-backfire antenna model for 3000 MHz ($\lambda = 10.0$ cm) is shown in Fig. 2(a). The diameter of

the larger reflector (*M*) is 2.0λ ; the smaller reflector (*R*) is a circular metal disk 0.4λ in diameter, spaced 0.5λ from the larger reflector. It offers the advantage of being insensitive to the polarization of the feed, which may consequently be linear in any direction, circular or crossed. The width of the rim surrounding reflector *M* is 0.25λ . Either reflector could be made from solid or perforated sheet material, or any other structural design equivalent in reflectivity.

The configuration of the short-backfire seems to be somewhat similar to that of the "reflex" antenna developed by G. v. Trentini [7]. However, the two antennas are based on quite different principles and also differ essentially in structure. The reflex antenna applies multiple reflection between a total reflector and a partial one of equal area that usually consists of a number of parallel metal rods or strips, the radiating aperture being defined by the structure and reflectivity of the partial reflector. In contrast the two reflectors of the short-backfire antenna (*M* and *R*) differ radically in area (area ratio between 15-to-1 and 30-to-1), with the smaller reflector (*R*) in its simplest form consisting of a solid metal disk; the radiating aperture forms in the area surrounding the smaller reflector and extends—undisturbed by metal rods or strips—even beyond the cross-sectional area of the larger reflector, as an experimental nearfield study has shown.

The gain of the short-backfire antenna of Fig. 2(a) was measured to be 13.1 dB above a dipole, or 15.2 dB above isotropic at 3000 MHz. Its 360° patterns in *E* and *H* plane are presented in Fig. 2(b). Rather remarkably, all sidelobes in the patterns are at least 20 dB below the maximum in the *E* as well as in the *H* plane, and the backlobe is far below 25 dB, the lowest level that shows in these patterns; further measurements indicated that it is in fact more than 30 dB below the maximum. These "clean" patterns were obtained over a frequency range of 1-to-1.4. Because the relatively high gain of the short-backfire is mainly due to the higher directivity in the *H* plane, this antenna type is especially suitable for the reception of horizontally polarized fields on or near ground.

The progress achieved with the new antenna structure can best be demonstrated by comparing it with the Yagi as the most frequently used endfire. A conventional Yagi with a gain of 15 dB isotropic has to be about 4.0λ long, and needs 15 to 20 dipole elements. The patterns of gain-optimized Yagis have relatively high sidelobes, however, especially in their *H*-plane patterns. To obtain patterns comparable to the low side—and backlobe patterns of the short-backfire, the number of reflectors and the axial length of the Yagi (number of directors) would have to be markedly increased, and the directors would require tapering to lower heights toward the radiating antenna termination. In Fig. 3 the short-backfire antenna (a) and Yagi (b), both constructed to have the same gain and about the same pattern quality, are shown to the same scaling factor so that they can be directly compared in size and material requirements. Although the reflector area of the short-backfire antenna is larger than that of the Yagi, and in addition a second small reflector is needed, the antenna length is less than one-tenth that of

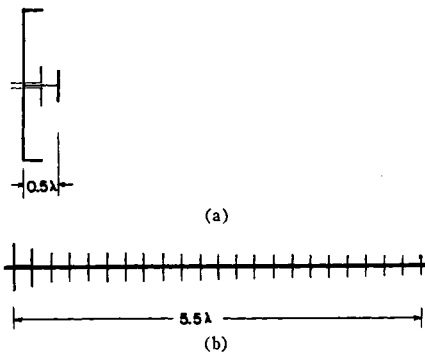


Fig. 3. Comparison of the physical structures of a short-backfire antenna and a Yagi with approximately the same patterns and gain (15 dB above isotropic). (a) Short-backfire antenna. (b) Yagi antenna.

the Yagi and the number of dipole elements is only 1 in contrast to 27 elements for the Yagi (including 5 reflector dipoles not shown).

H. W. EHRENSPECK
Air Force Cambridge Research Labs.
L. G. Hanscom Field,
Bedford, Mass.

REFERENCES

- [1] H. W. Ehrenspeck, "The Backfire Antenna, a New Type of Directional Line Source," *Proc. IRE (Correspondence)*, vol. 48, pp. 109-110, January 1960.
- [2] F. J. Zucker, "Surface and Leaky-Wave Antennas," in *Antenna Engineering Handbook*, H. Jasik, Ed. New York: McGraw-Hill, 1961, ch. 16.
- [3] H. W. Ehrenspeck, "Reflection Antenna Employing Multiple Director Elements and Multiple Reflection of Energy to Effect Increased Gain," U. S. Patent No. 3,122,745, February 1964. (Additional patents applied for.)
- [4] J. A. Strom and H. W. Ehrenspeck, "Backfire Antennas for SHF, UHF, and VHF Bands," AFCRL-63-114, AF Cambridge Research Labs., Bedford, Mass., April 1963.
- [5] H. W. Ehrenspeck, "The Backfire Antenna: New Results," *Proc. IEEE (Correspondence)*, vol. 53, pp. 639-641, June 1965.
- [6] F. J. Zucker, "The Backfire Antenna: A Qualitative Approach to its Design." To be published shortly.
- [7] G. v. Trentini, "Partially Reflecting Sheet Arrays," *IRE Trans. on Antennas and Propagation*, vol. AP-4, pp. 666-671, October 1956.

Automatic Equalization Using Time-Domain Equalizers

In recent months, some interesting articles on automatic, time-domain equalizers [1], [2] have appeared. This subject is considered highly important.¹ One purpose of this correspondence is to point out some earlier, less widely circulated reports [3]-[5] that discuss this subject in considerable detail and explain some additional, important considerations.

The type of equalizer under discussion consists basically of a delay line with adjustable taps. The general method of automating this equalizer described in recent references [1], [2] as well as by the writer [3]-[5] is based upon time-domain equa-

tions derived from the system pulse response by using simple superposition [3], [4]. This general method is interesting in theory, but has the following important disadvantages:

- 1) It depends upon utilizing samples of the system pulse response, including rather small parts of this response, in the presence of noise.
- 2) To measure or utilize these sample amplitudes, it is necessary to interrupt the flow of regular data long enough to transmit isolated pulses.

For automating the equalizer, a scheme that offers some important practical advantages has been described [5]. Briefly, a conventional "eye pattern" [2]-[4] (formed from the regular baseband signal on the face of an oscilloscope) is electronically scanned. Each potentiometer of the equalizer is automatically adjusted for the best "eye" opening, the signal from the scanner being used as an error signal in a servo-type arrangement used to drive the potentiometer. The potentiometers are adjusted sequentially in the order of decreasing expected effect upon the eye pattern. The advantages of this approach include the following:

- 1) The equalizer can be automatically adjusted in the presence of relatively poor signal-to-noise and high pre-equalization distortion.
- 2) The measurement errors can be largely averaged out, thus increasing the accuracy of equalization.
- 3) Equalization from the regular baseband signal alone. No need to transmit special pulses for equalization. The equalization process can proceed continually while data is being transmitted. The latter advantage could possibly make it feasible to correct time-varying frequency-selective fading, such as that caused by multipath in some types of radio systems. The oscilloscope can be replaced by basically similar methods of scanning the baseband signal.

The same reference [5] also describes some variations of this method of implementing the automation of the equalizers, including a method for use when the transmitted signal is unknown and there is no opening of the "eye pattern" prior to equalization.

This type of equalizer with manual adjustments has been used since early 1961 in the first known multiple-level vestigial-sideband suppressed-carrier data modem² and has proven highly versatile and accurate [4], [5].

Some examples of other important considerations previously discussed in detail [3]-[5] are:

- 1) Time-domain analyses which show a number of important relationships, including matrices inherently well suited for digital implementation of the automatic equalization.
- 2) Frequency-domain analyses that show, for example, that when the phase-frequency curve nonlinearity can be approximated by a sine wave, $B \sin \omega t$, the proper settings of the potentiometers are:

$$G_0 = 2J_0(B)$$

$$G_n = G_{-n} = J_n(B), n \text{ even}$$

$$G_n = G_{-n} = -J_n(B), n \text{ odd},$$

where $J_n(B)$ is the Bessel function of the first kind of order n and G_n is the gain setting for the n th tap numbered from the middle of the delay line. These analyses also show the high versatility obtainable from this type of equalizer, as well as estimates of the range and accuracy obtainable from limited numbers of stages [3], [4].

3) Determination of critical combinations of bits or other signaling elements, i.e., those resulting in the maximum distortion, or maximum positive and negative error in signal amplitude [3].

4) Schemes for ganging the potentiometers to reduce the number of adjustments under certain conditions [3].

5) Use of a shift register to replace the delay line, especially for shaping the signal prior to transmission [3].

6) Considerations involved in letting the sampling interval equal the signal element duration ("interbit adjustment" equalization) [3].

7) The number of equalizer stages required for some typical applications. For example, in agreement with results now reported by Rapoport [1], six stages were reported as adequate for most telephone line applications [3].

The writer can offer interested readers copies of references [3]-[5] to a limited extent.

EARL D. GIBSON
Radar and Communications Dept.
Aerospace Corp.
San Bernardino, Calif.

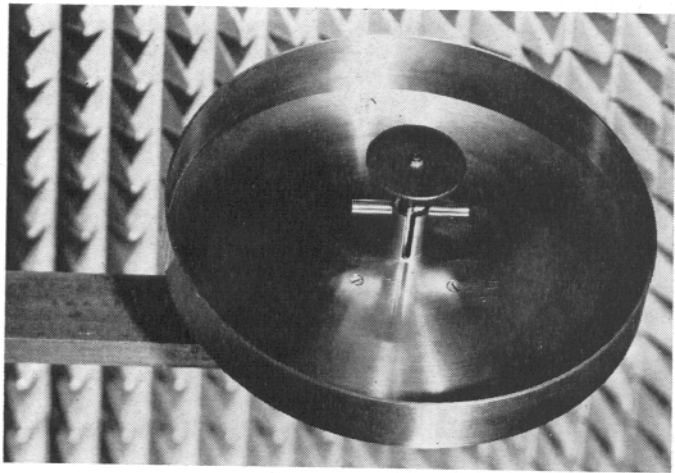
REFERENCES

- [1] M. A. Rapoport, "Automatic equalization of data transmission facility distortion using transversal equalizers," *IEEE Transactions on Communications Technology*, vol. COM-12, pp. 65-73, September 1964.
- [2] F. K. Becker, et al., "Automatic equalization for digital communications," *Proc. IEEE*, vol. 53, pp. 96-97, January 1965.
- [3] E. D. Gibson, "An intersymbol adjustment method of distortion compensation," *Proc. MIL-E-CON*, Washington, D. C., pp. 196-207, June 1961.
- [4] E. D. Gibson, "A highly versatile corrector of distortion and impulse noise," 1961 *Proc. NEC*, pp. 543-556.
- [5] E. D. Gibson and W. G. Burke, Jr., "Automatic equalization of standard voice telephone lines for digital data transmission," ACF Industries, ACFE Rept. 88-0275-101, August 1961.

On the Brown-Twiss Circuit

In a recent communication [1], Chen and van der Ziel propose the Brown-Twiss radiometer circuit (Fig. 1) [2] for measuring the power level of weak noise sources. The purpose of the present note is three-fold: first to remark that the proposed application has been known for some years, second to point out that the circuit possesses optimal properties for power level measure-

² Four ACF Industries patents by E. D. Gibson pending on the modem and equalizer. This was the first known data modem capable of achieving 4800 bits per second over a wide variety of ordinary telephone lines, and this is the same type of application discussed in Rapoport [1], and Becker, et al. [2].



(a)